Polarization-Selective and Wide-Angle Photodetector Based on Resonant Waveguide Grating

Hu Jinhua Huang Yongqing Duan Xiaofeng Wang Qi Zhang Xia
Shang Yufeng Ren Xiaomin

(*State Key Laboratory of Information Photonics and Optical Communications*, *Institute of Information Photonics and Optical Communications*, *Beijing University of Posts and Telecommunications*, *Beijing* 100876, *China*)

Abstract A polarization-selective photodetector with high performance is necessary for polarization sensitive systems. A hybrid integrated photodetector is proposed by integrating a silicon resonant waveguide grating with an InP/InGaAs PIN photodetector. The resonant waveguide grating is designed using rigorous coupled-wave analysis method. Parameters of the hybrid integrated photodetector are optimized by finite difference time domain method. The simulated results indicate that the proposed photodetector exhibits high quantum efficiency, large incident angle tolerance, and polarization selectivity in a broad spectral range, which can be used in polarization sensitive systems.

Key words optical devices; polarization-selective device; wide angle; resonant waveguide grating; photodetector

OCIS codes 230.5160; 230.5440; 050.2770

基于谐振波导光栅的偏振选择广角光探测器

胡劲华 黄永清 段晓峰 王 琦 张 霞 尚玉峰 任晓敏

(北京邮电大学信息光子学与光通信研究院信息光子学与光通信国家重点实验室, 北京 100876)

摘要 高性能偏振选择型光探测器是偏振检测系统中不可或缺的一部分。提出了一种由硅基谐振波导光栅和InP/InGaAs PIN光探测器混合集成的光探测器结构。利用严格耦合波分析方法设计了硅基谐振波导光栅结构，利用时域有限差分法优化了该混合集成光探测器的结构参数。数值仿真结果表明该光探测器在宽带范围内具有高量子效率、较大入射角容差及偏振选择性。该器件可以应用于偏振敏感系统中。

关键词 光学器件；偏振选择；广角；谐振波导光栅；光探测器

中图分类号 O436 **文献标识码** A **doi**: 10.3788/CJL201441.0405005

1 Introduction

Polarization-selective (PS) photodetectors have been widely used in polarization sensitive systems[1-3]. Several integrated devices can be used as polarization-selective photodetectors, such as metal grating[2], photonic crystal[3], and so on. However, some disadvantages exist in conventional polarization-selective photodetectors. For example, metal grating photodetector needs high cost; photonic crystal photodetector needs elaborate fabrication. These disadvantages restrict further applications of polarization-selective photodetectors.

In recent years, resonant waveguide grating (RWG) has emerged as a significant functional device for photonic integrated circuits due to its unique properties and structural simplicity[4-5]. Several functional components have been reported using silicon RWG structures, such as angular bandpass filters[6], broadband reflective mirrors[7], broadband non-polarizing beam splitter[8] and optical sensors[9]. Silicon RWG exhibits great advantage in terms of loss, polarization sensitivity and reflection over metal grating and multi-layer stacks. Therefore, silicon RWG is a better candidate for polarization selection component for photodetectors. However, the reflectivity of silicon

收稿日期: 2013-10-29; **收到修改稿日期**: 2013-11-26

基金项目: 国家 973 计划(2010CB327600)、国家自然科学基金(61020106007,61274044)、北京市自然科学基金(4132069)

作者简介: 胡劲华(1984—),男,博士研究生,主要从事半导体光电子器件及其光通信网络方面的研究。E-mail: hujh84@gmail.com

导师简介: 任晓敏(1958—),男,教授,博士生导师,主要从事半导体光电子器件方面的研究。E-mail: xmren@bupt.edu.cn

RWG is typically sensitive to the incident angle[10]. In order to achieve high efficient photo detection, we should enhance the angle tolerances of the incident light.

Silicon is an excellent material for passive components. However, it is not very suitable for the application of active components because of the intrinsic limit. That is to say, silicon is an indirect bandgap material, which cannot be directly used in detection and generation of light at communication wavelengths (1.3 ~ 1.5 μm). Compared with silicon materials, Ⅲ-Ⅴ semiconductor materials behave much better in active functional devices[11]. Currently, the hybrid integration of Si/Ⅲ-Ⅴ semiconductor materials is a practicable solution by integrating silicon passive photonics with Ⅲ-Ⅴ semiconductor materials for optical devices[12-14].

In this paper, we propose a new type of photodetector by integrating silicon resonant waveguide grating with InP/InGaAs PIN photodetector structure, which has polarization selectivity and large incident angle tolerance. We design a resonant waveguide grating structure by using rigorous coupled-wave analysis (RCWA) method[15-16] and modelling method[17]. Finite difference time domain (FDTD) method is used to evaluate the behavior of the hybrid integrated photodetector. After optimization, the photodetector achieves high quantum efficiency from 1.4 μm to 1.6 μm for TM-polarized light. Compared with traditional photodetectors, the new type of photodetector is more compact and has wider-angle. It can be used for polarization photo detection with higher integrated level in polarization sensitive systems.

2 Structure and Design

Figure 1 is the schematic diagram of the hybrid integrated photodetector structure. The device consists of a silicon resonant waveguide grating, a benzocyclobutene (BCB) bonding layer, and an InP/InGaAs PIN photodetector. The hybrid integrated photodetector is bottom-incident type. That is to say, the incident light couples into the PIN photodetector absorption layer through the RWG and the BCB bonding layer. Figure 2 is the schematic diagram of the RWG, which consists of a silicon layer and a silica layer. With special design of the RWG structure, the resonant grating will exhibit selection for TM- and TE-polarized light at wide incident angle operating in broadband.

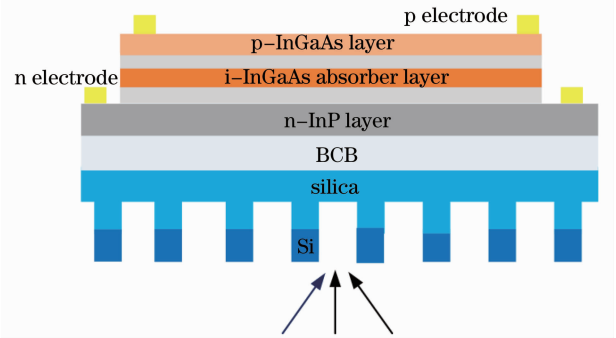

Fig. 1 Schematic diagram of the hybrid integrated photodetector structure

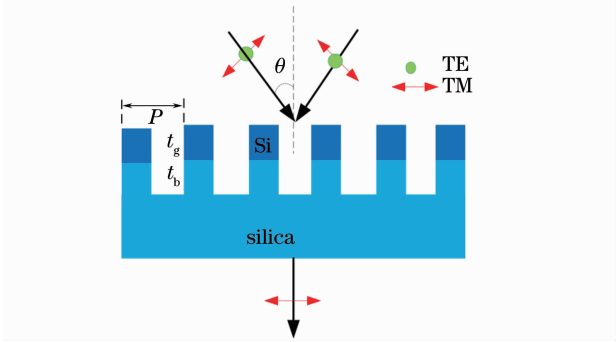

Fig. 2 Schematic diagram of RWG

In our simulation, the thicknesses of the silicon grating layer and the silica grating layer are denoted as t_g and t_b, respectively. The grating period is P, the grating duty cycle is f_d, the angle of the desired transmission range is θ. The thicknesses of the BCB bonding layer and the i-InGaAs absorbing layer are denoted as t_{BCB} and t_{ab}, respectively. The refractive indices of the amorphous silicon (a-Si) and the silica layer are $n_H = 3.48$ and $n_L = 1.48$ (at $\lambda = 1550$ nm), respectively.

In order to combine high efficiency transmission and wide incident angle in broadband, the desired angle of the transmission range should satisfy the folowing relation[6]

$$\frac{\lambda}{n_L + \sin\theta} < P < \frac{\lambda}{n_L}. \tag{1}$$

According to the Eq. (1), if we choose the desired angle of the transmission range as 30°, the grating period P will be limited in the range from 0.78 μm to 1.407 μm. In the following discussion, we choose the grating period P as 0.85 μm. It means that the first order diffraction light could propagate in the RWG structure. Physically, there will be two propagating resonant modes excited in grating layer. The two modes will interfere with each other. The phase difference of the two different modes could be changed with the thickness of grating layer. In the PS-RWG structure, the silicon grating with high transmission could be designed for the normal-incident TM-polarized light and high reflection for the normal-incident TE-polarized light.

According to the modelling theory proposed by Botten *et al.*[17], the thickness of the amorphous silicon grating layer t_g could be calculated by

$$\begin{cases} t_g = \dfrac{\lambda m}{n_{\mathrm{eff}_0}^{\mathrm{TM}} - n_{\mathrm{eff}_1}^{\mathrm{TM}}} \\ t_g = \dfrac{\lambda(2m+1)}{2(n_{\mathrm{eff}_0}^{\mathrm{TE}} - n_{\mathrm{eff}_1}^{\mathrm{TE}})} \end{cases}, \quad m \in N, \tag{2}$$

where n_{eff_0} and n_{eff_1} are effective refractive indices of two modes for TE- or TM-polarized light (at $\lambda = 1550$ nm). The thickness of silicon grating layer t_g ranges from 124 nm to 303 nm. In order to design a polarization-selective RWG structure with wide angular transmission, we choose the depth of the silicon grating layer t_g as 220 nm. We calculate the spectrum of this structure for both TE- and TM-polarized light at normal incidence using RCWA method. As a result, the thickness of silica grating layer and the duty cycle for the RWG are obtained at $t_b = 200$ nm and $f_d = 0.28$, respectively.

We investigate the spectrum responses of the RWG structure for different incident angles at the wavelength ranged from 1.4 μm to 1.6 μm for TE- and TM-polarized light using RCWA method. The results are shown in Fig. 3. Figure 3(a) is the transmission spectrum of TM-polarized light while Fig. 3(b) is the reflection spectrum of TE-polarized light. From the simulation result, we can see that the angular bandwidth is 40° ranging from −20° to 20° for TM-polarized light. On the other hand, the angular bandwidth is 20° ranging from −10° to 10° for TE-polarized light. We obtain that the transmission for TM-polarization is larger than 87% with the incident angle ranging from 0° to 20°, while the reflection for TE-polarization is larger than 76% with the incident angle ranging from 0° to 10°.

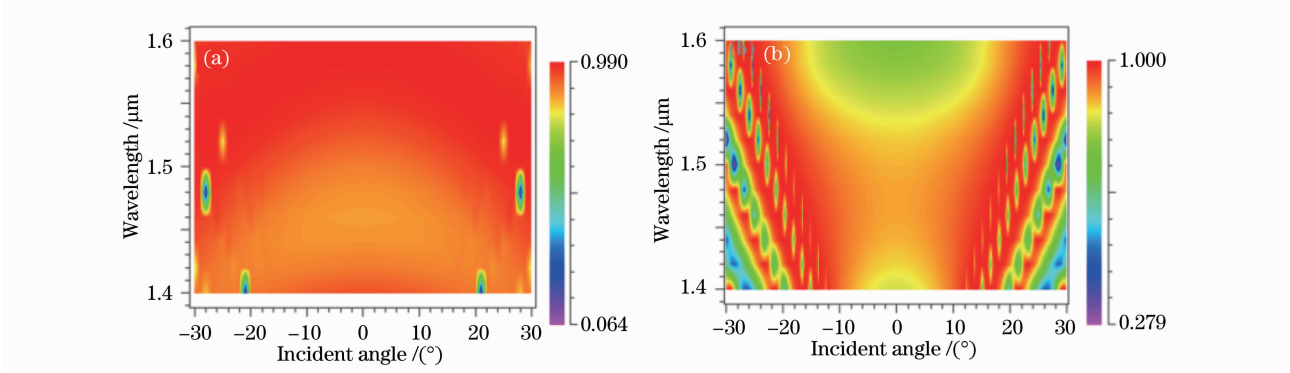

Fig. 3 Spectrum responses of the PS-RWG structure for different incident angles at the wavelength range from 1.4 μm to 1.6 μm for TM- and TE-polarized lights. (a) Transmission spectrum for TM-polarized light; (b) reflection spectrum for TE-polarized light

3 Results and Discussion

The parameters of the hybrid integrated photodetector are shown in Table 1. Our InP/InGaAs PIN photodetector structure is similar to the PIN photodetector structure in Ref. [12]. In order to improve the quantum efficiency of the hybrid integrated photodetector, we will optimize the the thicknesses of the BCB bonding layer t_{BCB} and the i-InGaAs absorbing layer t_{ab}.

Table 1 Parameters of the hybrid integrated photodetector

Structure	Thickness /nm	Index
InP n contact layer	300	3.17
InGaAs etch layer	40	3.56
InP spacer layer	470	3.17
InGaAs absorbing layer	t_{ab}	3.60 − i0.0965
InP spacer layer	240	3.17
InGaAs p contact layer	200	3.56
BCB bonding layer	t_{BCB}	1.54
Silicongrating layer	220	3.48
Silica grating layer	200	1.48

We simulate the quantum efficiency of the hybrid integrated photodetector by FDTD method, as shown in Fig. 4. We investigate the quantum efficiency as a function of the thickness of i-InGaAs absorbing layer for different BCB thicknesses. We can see that the quantum efficiency spectrum has a resonant trend, which is caused by phase-matching of different order modes in PIN waveguide and the transmission mode inthe RWG.

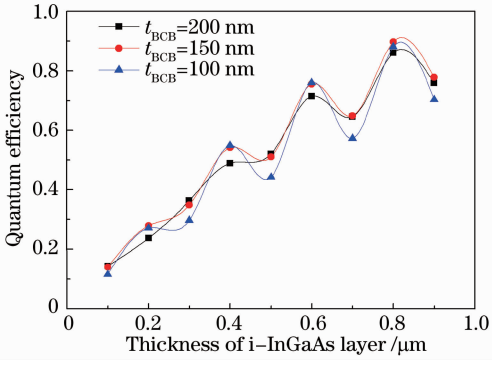

Fig. 4 Quantum efficiency of the hybrid integrated photodetector as a function of the thickness of the i-InGaAs absorbing layer

The quantum efficiency has some peaks with the thicknesses of i-InGaAs absorbing layer of 200, 400, 600 nm, respectively. From the simulation result, we can see that we could choose the thicknesses of the BCB bonding layer and the i-InGaAs absorbing layer as t_{BCB} = 150 nm and t_{ab} = 600 nm, respectively, to obtain a high quantum efficiency.

In order to investigate the effect of the incident angle, we simulate the quantum efficiency of the hybrid integrated photodetector at different incident angles for TM-polarized light at the wavelength of 1550 nm by FDTD method. The result is shown in Fig. 5. From this figure, one can see that when the incident angle of TM-polarized light varies from −30° to 30°, the quantum efficiency reaches 70% with a flat top angular response.

We simulate the optical field intensity distributions in the hybrid integrated photodetector for TM- and TE-polarized light by FDTD method, as shown in Figs. 6(a) and (b), respectively. Figure 6(a) presents that there is a high transmission for TM-polarized light. This phenomenon is caused by resonant waveguide grating. Optical absorption can be observed in the i-InGaAs absorbing layer. Meanwhile, the TE-polarized light is reflected by the resonant waveguide grating structure, as shown in Fig. 6(b). The simulated results show that the resonant waveguide grating exhibits excellent polarization selection for TE- and TM-polarized lights at normal incidence.

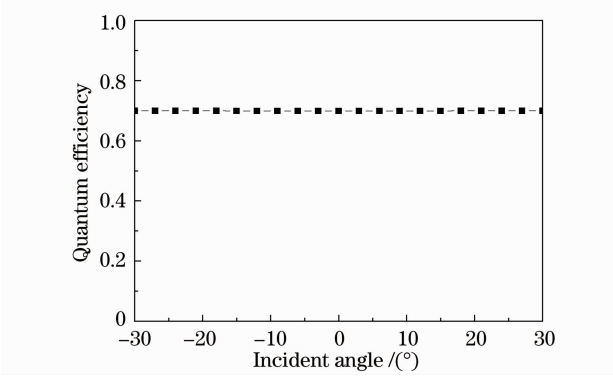

Fig. 5 Quantum efficiency of the hybrid integrated photodetector as a function of the incident angle simulated by FDTD method

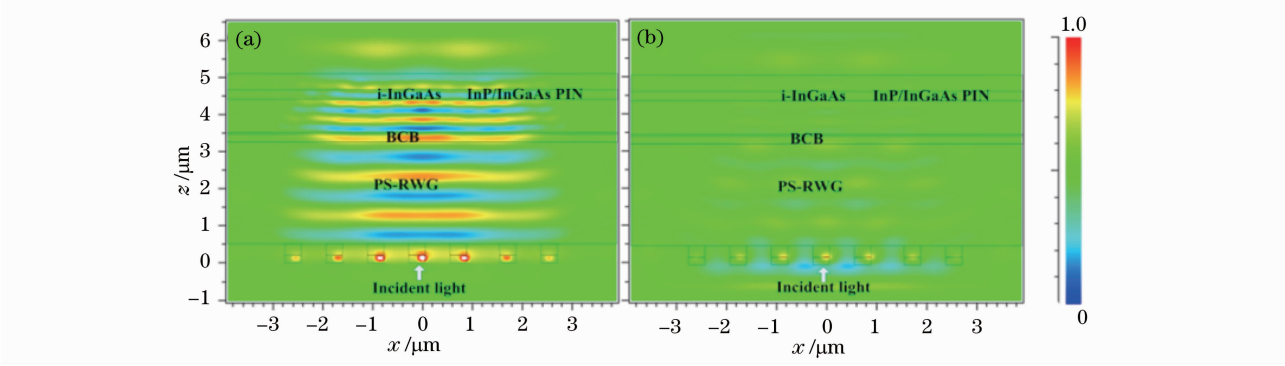

Fig. 6 Optical field intensity distribution of the hybrid integrated photodetector for two different polarized lights at the wavelength of 1550 nm. (a) TM-polarized light; (b) TE-polarized light

Finally, we also simulate the optical wavelength response of the designed hybrid integrated photodetector for TM-polarized light at different incident angles using the same method, as shown in Fig. 7. From this figure, we can see that the quantum efficiency of the photodetector is about 70% at different incident angles in a broad spectra range (from 1.4 μm to 1.6 μm) for TM-polarized light.

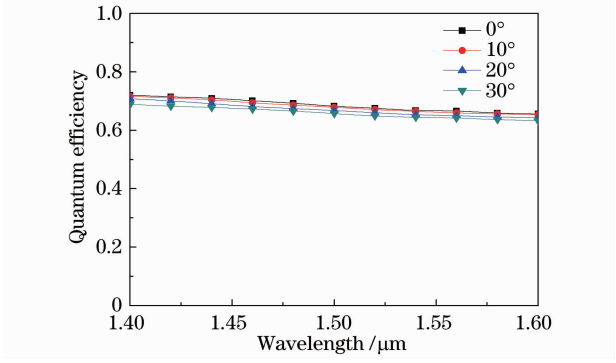

Fig. 7 Quantum efficiency of the hybrid integrated photodetector as a function of wavelength for TM-polarized light at different incident angles

4 Conclusion

In conclusion, we have designed a hybrid integrated photodetector, which has selectivity for two different polarized lights. We investigate the effects of different parameters of the structure on the quantum efficiency of the hybrid integrated photodetector. The simulation results show that the hybrid integrated photodetector has polarization detection ability with large angular tolerance in a wide optical spectral range. This integrated photodetector could be used for polarization detection in optical polarization sensitive systems.

References

1 Deri R J, Pennings E C M, Scherer A, *et al*.. Ultracompact

monolithic integration of balanced, polarization diversity photodetectors for coherent lightwave receivers[J]. IEEE Photon Technol Lett, 1992, 4(11): 1238 - 1240.

2 Apalkov V, Ariyawansa G, Unil Perera A G, *et al*.. Polarization sensitivity of quantum well infrared photodetector coupled to a metallic diffraction grid [J]. IEEE J Quantum Electron, 2010, 46(6): 877 - 883.

3 Yang J K, Seo M K, Hwang I K, *et al*.. Polarization-selective resonant photonic crystal photodetector [J]. Appl Phys Lett, 2008, 93(21): 211103.

4 Ding Y, Magnusson R. Resonant leaky-mode spectral-band engineering and device applications [J]. Opt Express, 2004, 12(23): 5661 - 5674.

5 Yang Yisu, Huang Yongqing, Huang Hui, *et al*.. Design of photodetector with subwavelength grating structure[J]. Chinese J Lasers, 2009, 36(9): 2352 - 2357.
杨一粟, 黄永清, 黄 辉, 等. 一种具有亚波长光栅结构的光探测器的设计[J]. 中国激光, 2009, 36(9): 2352 - 2357.

6 Steiner S, Kroker S, Käsebier T, *et al*.. Angular bandpass filters based on dielectric resonant waveguide gratings[J]. Opt Express, 2012, 20(20): 22555 - 22562.

7 Mateus C F R, Huang M C Y, Chen L, *et al*.. Broad-band mirror (1.12 ~ 1.62 μm) using a subwavelength grating [J]. IEEE Photon Technol Lett, 2004, 16 (7): 1676 - 1678.

8 Ma Jianyong, Xu Cheng, Qiang Yinghuai, *et al*.. Broadband non-polarizing beam splitter based on guided mode resonance effect [J]. Chin Phys B, 2011, 20(10): 104209.

9 Schmid J H, Sinclair W, García J, Janz S, *et al*.. Silicon-on-insulator guided mode resonant grating for evanescent field molecular sensing [J]. Opt Express, 2009, 17(20): 18371 - 18380.

10 Jacob D K, Dunn S C, Moharam M G. Normally incident resonant grating reflection filters for efficient narrow-band spectral filtering of finite beams[J]. J Opt Soc Am A, 2001, 18 (9): 2109 - 2120.

11 Roelkens G, Thourhout D V, Baets R. Laser emission and photodetection in an InP/InGaAsP layer integrated on and coupled to a silicon-on-insulator waveguide circuit[J]. Opt Express 2006, 14(18): 8154 - 8159.

12 Fan X Y, Huang Y Q, Ren X M, *et al*.. Hybrid integrated photodetector with flat-top steep-edge spectral response[J]. Appl Opt, 2012, 51(24): 5767 - 5772.

13 Sheng Z, Liu L, Brouckaert J, *et al*.. InGaAs PIN photodetectors integrated on silicon-on-insulator waveguides[J]. Opt Express , 2010, 18(2): 1756 - 176.

14 Huang Hui, Ren Xiaomin, Lü Jihe, *et al*.. Monolithically integrated Si-based wavelength-selective photodetector operating at long wavelength[J]. Chinese J Lasers, 2009, 36(s1): 356 - 359.
黄 辉, 任晓敏, 吕吉贺, 等. 具有波长选择功能的单片集成 Si 基波长光探测器[J]. 中国激光, 2009, 36(s1): 356 - 359.

15 Moharam M G, Pommet D A, Grann E B. Stable implementation of the rigorous coupled-wave analysis for surface-relief gratings: enhanced transmittance matrix approach[J]. J Opt Soc Am A, 1995, 12(5): 1077 - 1086.

16 Moharam M G, Grann E B, Pommet D A. Formulation for stable and efficient implementation of the rigorous coupled-wave analysis of binary gratings[J]. J Opt Soc Am A, 1995, 12(5): 1068 - 1076.

17 Botten I C, Craig M S, McPhredran R C, *et al*.. The dielectric lamellar diffraction grating[J]. Opt Act, 1981, 28(3): 413 - 428.

栏目编辑: 宋梅梅